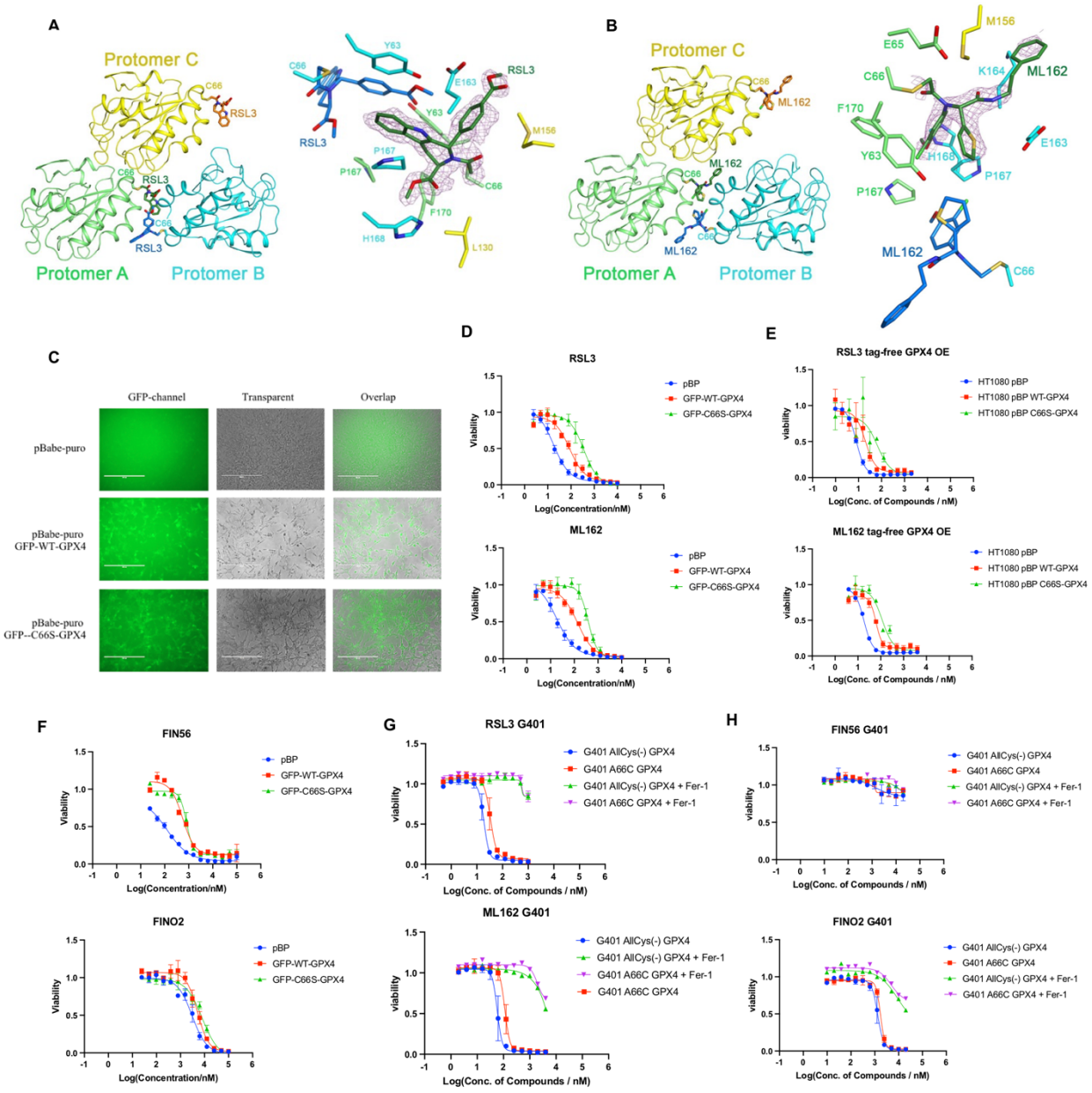

Supplemental Figure 1. Region around Cysteine 66 is a binding site of RSL3 and ML162 on GPX4, Related to Figure 1. **A**, A cartoon representation of the three protomers of GPX4^{U46C} in complex with RSL3 is shown in the panel on the left. The three protomers (light green, cyan, and yellow), the RSL3 molecules (dark green, marine, and orange), and the side chains of amino acids cys66 are shown with stick models and labeled. A close-up view of the two RSL3 molecules (dark green and marine) at the interface of protomer A and protomer B was shown in the panel on the right, along with the side chains of residues that are involved in recognition of the RSL3 (dark green) from protomer A (light green). The Fo-Fc omit map, contoured at 3σ (in grey mesh), for the RSL3 molecule (dark green) from the protomer A (light green) is also shown and all the involved residues are labeled with respective color codes. **B**, A cartoon representation of the three protomers of GPX4$^{U46C\text{-}R152H}$ in complex with ML162 is shown in the panel on

the left. The three protomers (light green, cyan, and yellow), the ML162 molecules (dark green, marine, and orange), and the side chains of amino acids cys66 are shown with stick models and labeled. A close-up view of the two ML162 molecules (dark green and marine) at the interface of protomer A and protomer B was shown in the panel on the right, along with the side chains of residues that are involved in recognition of the ML162 (dark green) from protomer A (light green). The Fo-Fc omit map, contoured at 3σ (in purple mesh), for the ML162 molecule (dark green) from the protomer A (light green) is also shown and all the involved residues are labeled with respective color codes. **C**, HT1080 transfected with pBabepuro (pBP) empty vector, pBP GFP-cGPX4^{WT}, and pBP GFP-cGPX4^{C66S} were selected with puromycin and imaged with microscope. The indicated white scale bar is 400 μm. **D**, HT1080 cells overexpressing GFP-GPX4^{WT} or GFP-GPX4^{C66S} and HT1080 cells transfected with pBabepuro (pBP) empty vector were tested for sensitivities to RSL3 and ML162. Viability was normalized to DMSO control of each line (n=3). **E**, HT1080 cells overexpressing tag-free GPX4^{WT} or GPX4^{C66S} and HT1080 cells transfected with pBabepuro (pBP) empty vector were tested for sensitivities to RSL3 in a 12-point response curve starting from 2 μM and ML162 in a 11-point response curve starting from 4 μM. Viability was normalized to DMSO control of each line (n=3). **F**, HT1080 cells overexpressing GFP-GPX4^{WT} or GFP-GPX4^{C66S} and HT1080 cells transfected with pBabepuro (pBP) empty vector were tested for sensitivities to FIN56 and $FINO_2$. Viability was normalized to DMSO control of each line (n=3). **G** and **H**, G401 cells overexpressing GFP-GPX4$^{AllCys(-)}$ or GFP-GPX4$^{AllCys(-)\ A66C}$ were tested for sensitivities to RSL3, ML162, FIN56, and $FINO_2$ in a 12-point response curve starting from 1 μM (RSL3), 4 μM (ML162), or 20 μM (FIN56 and $FINO_2$). Ferrostatin-1 (Fer-1) is a ferroptosis-specific inhibitor (Dixon et al., 2012). Fer-1 rescue was included to confirm the observed cell death to be ferroptosis. Viability was normalized to DMSO control of each line (n=3). All viability data were based on CellTiter-Glo assay. Data in **D**-**H** are represented as mean ± s.d.

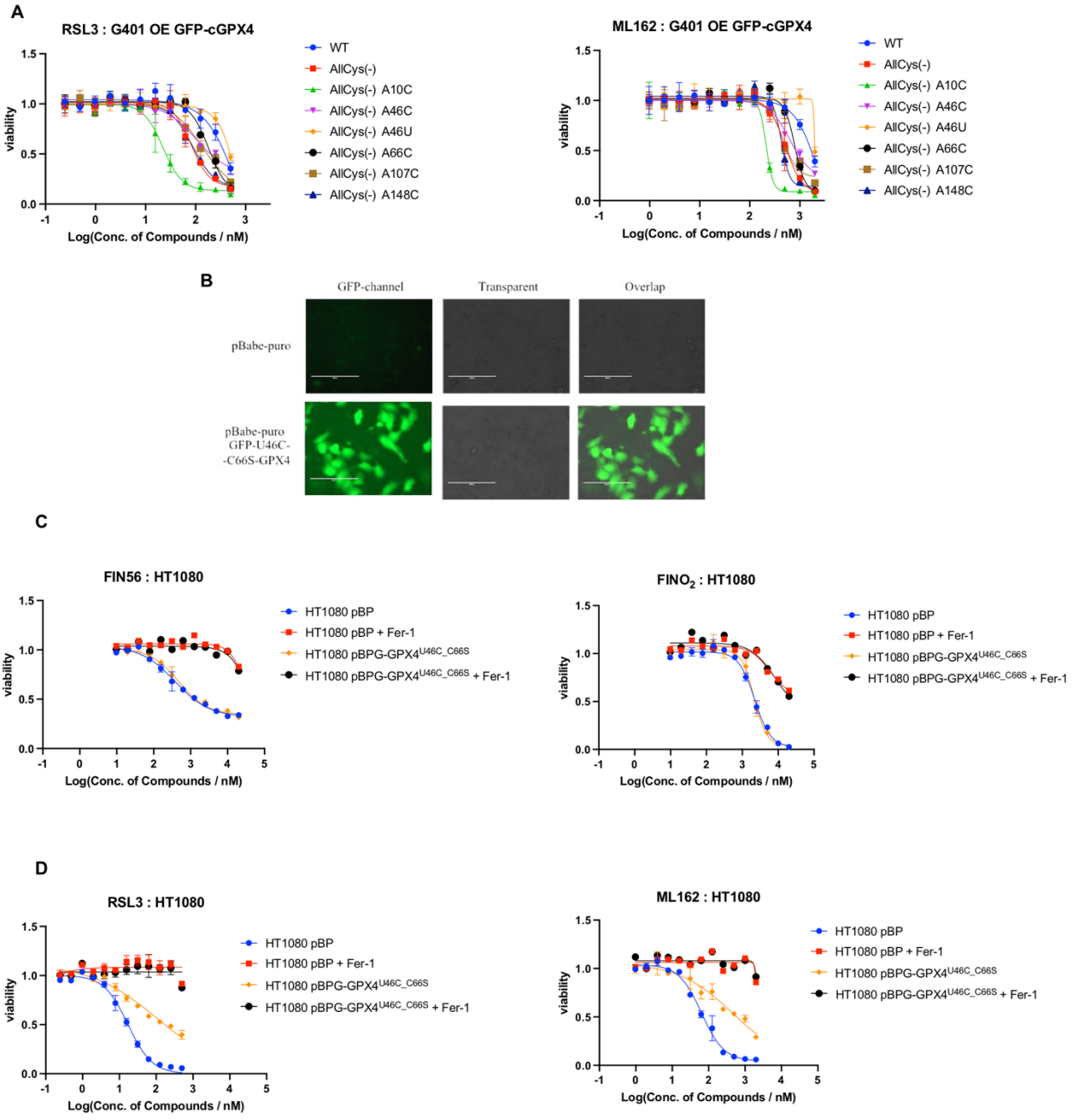

Supplemental Figure 2. RSL3 and ML162 specifically bind to Sec46 and Cys66 of GPX4, Related to Figure 2. A, G401 overexpressing GFP-tagged WT, allCys(-), allCys(-) A10C, allCys(-) A46C, allCys(-) A46U, allCys(-) A66C, allCys(-) A107C, and allCys(-) A148C GPX4 were tested for sensitivities to RSL3 in a 12-point response curve starting from 0.5 μM and ML162 in a 12-point response curve starting from 2 μM (n=3). Viability normalized to DMSO control of each line. **B**, HT1080 transfected with pBabepuro (pBP) empty vector or pBP GFP-cGPX4$^{U46C-C66S}$ were selected with puromycin and imaged with microscope. The indicated white scale bar is 200 μm. **C** and **D**, HT1080 cells overexpressing GFP-GPX4$^{U46C-66S}$ and HT1080 cells transfected with pBabepuro (pBP)

empty vector were tested for sensitivities to FIN56, $FINO_2$, RSL3, and ML162 in a 12-point response curve starting from 20 μM, 20 μM, 0.5 μM, and 2 μM, respectively (n=3). Viability was normalized to DMSO control of each line. All viability data were based on CellTiter-Glo assay. Data in **A, C,** and **D** are represented as mean ± s.d.

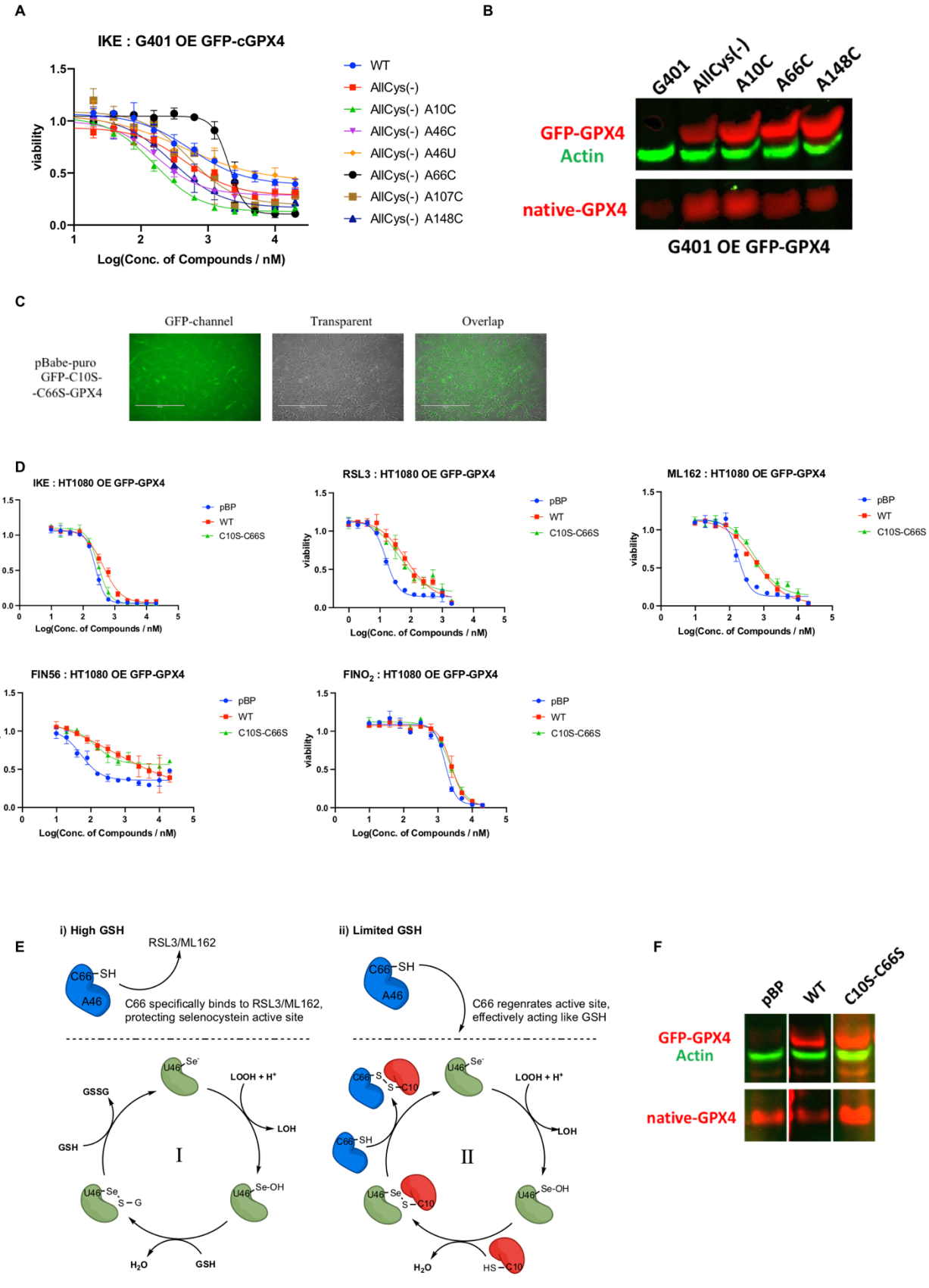
A
IKE : G401 OE GFP-cGPX4
viability
Log(Conc. of Compounds / nM)
WT
AllCys(-)
AllCys(-) A10C
AllCys(-) A46C
AllCys(-) A46U
AllCys(-) A66C
AllCys(-) A107C
AllCys(-) A148C
B
G401
AllCys(-)
A10C
A66C
A148C
GFP-GPX4
Actin
native-GPX4
G401 OE GFP-GPX4
C
GFP-channel
Transparent
Overlap
pBabe-puro
GFP-C10S-
-C66S-GPX4
D
IKE : HT1080 OE GFP-GPX4
RSL3 : HT1080 OE GFP-GPX4
ML162 : HT1080 OE GFP-GPX4
FIN56 : HT1080 OE GFP-GPX4
FINO2 : HT1080 OE GFP-GPX4
pBP
WT
C10S-C66S
viability
Log(Conc. of Compounds / nM)
E
i) High GSH
RSL3/ML162
C66–SH
A46
C66 specifically binds to RSL3/ML162,
protecting selenocystein active site
ii) Limited GSH
C66 regenrates active site,
effectively acting like GSH
U46–Se⁻
LOOH + H⁺
LOH
GSSG
GSH
U46–Se–S–G
U46–Se-OH
H2O
I
II
C66–S–S–C10
HS–C10
U46–Se–S–C10
F
pBP
WT
C10S-C66S
GFP-GPX4
Actin
native-GPX4

Supplemental Figure 3. Cys66 and Cys10 are involved in modulating the dual function of GPX4, Related to Figure 3. A, G401 overexpressing GFP-tagged WT, allCys(-), allCys(-) A10C, allCys(-) A46C, allCys(-) A46U, allCys(-) A66C, allCys(-) A107C, and allCys(-) A148C GPX4 were tested for sensitivities to IKE. Viability normalized to DMSO control of each line. Data are represented as mean ± s.d. (n=3). **B**, Western blot of G401 and G401 overexpressing allCys(-), allCys(-) A10C, allCys(-) A66C, or allCys(-) A148C GPX4 with GPX4 and actin antibodies. **C**, HT1080 transfected with pBabepuro (pBP) empty vector, pBP GFP-cGPX4^{U46C}, and pBP GFP-cGPX4$^{U46C-C66S}$ were selected with puromycin and imaged with microscope. The indicated white scale bar is 400 μm. **D**, HT1080 cells overexpressing GFP-GPX4^{WT} or GFP-GPX4$^{C10S-C66S}$ and HT1080 cells transfected with pBabepuro (pBP) empty vector were tested for sensitivities to IKE, ML162, FIN56, and $FINO_2$. Viability was normalized to DMSO control of each line. All viability data were based on CellTiter-Glo assay. Data are represented as mean ± s.d. (n=3). **E**, A cartoon model demonstrating the different protective or activation effect of C66 site under high/regular GSH condition or limited GSH condition. **F**, Western blot of HT1080 pBP (empty vector) and HT1080 overexpressing WT or C10S-C66S GPX4 with GPX4 and actin antibodies.

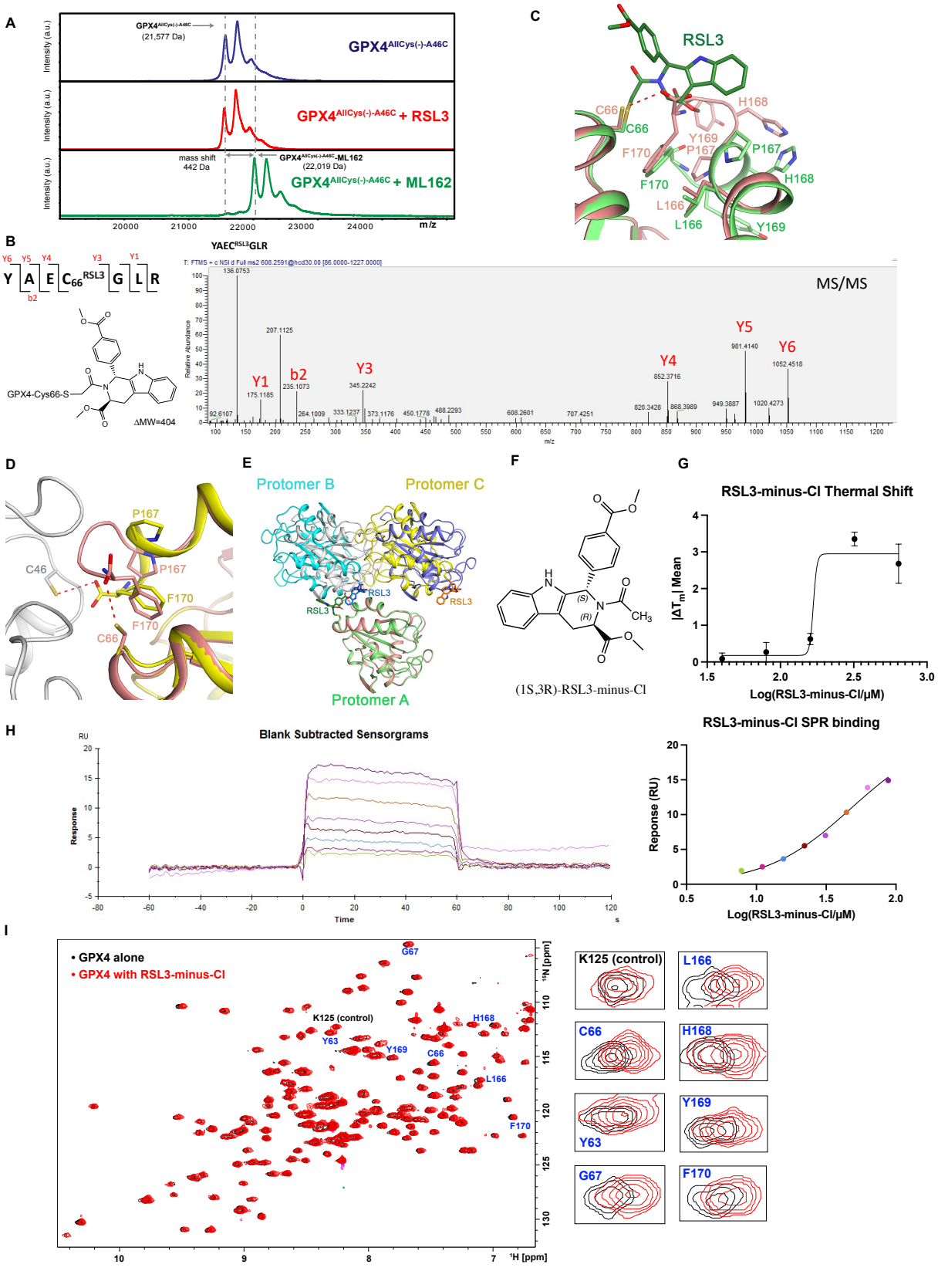
A
GPX4AllCys(-)-A46C
(21,577 Da)
GPX4AllCys(-)-A46C
GPX4AllCys(-)-A46C + RSL3
mass shift
442 Da
GPX4AllCys(-)-A46C-ML162
(22,019 Da)
GPX4AllCys(-)-A46C + ML162
Intensity (a.u.)
m/z
B
YAECRSL3GLR
Y6 Y5 Y4 Y3 Y1
b2
GPX4-Cys66-S
ΔMW=404
MS/MS
Y1
b2
Y3
Y4
Y5
Y6
Relative Abundance
m/z
C
RSL3
C66
H168
Y169
P167
F170
L166
D
P167
C46
F170
C66
E
Protomer B
Protomer C
Protomer A
RSL3
F
(1S,3R)-RSL3-minus-Cl
G
RSL3-minus-Cl Thermal Shift
|ΔTm| Mean
Log(RSL3-minus-Cl/μM)
H
Blank Subtracted Sensorgrams
RU
Response
Time
RSL3-minus-Cl SPR binding
Reponse (RU)
Log(RSL3-minus-Cl/μM)
I
• GPX4 alone
• GPX4 with RSL3-minus-Cl
K125 (control)
G67
H168
Y63
Y169
C66
L166
F170
¹⁵N [ppm]
¹H [ppm]
K125 (control)
L166
C66
H168
Y169
Y63
G67
F170

Supplemental Figure 4. Analysis of the binding of RSL3 and its non-covalent analogue RSL3-minus-Cl to GPX4 , Related to Figure 4. A, Intact protein MALDI MS of $GPX4^{AllCys(-)-A46C}$ preincubated with DMSO, RSL3, or ML162. **B**, LC–MS/MS spectra of the RSL3 modification of $GPX4^{U46C}$ at residue C66. In the LC-MS/MS analysis on trypsin digested $GPX4^{U46C}$-RSL3 complex, the peptide containing Cysteine 66 (YAECGLR) was analysed for mass shift induced by binding of RSL3 (404.14). **C,** Structural overlay of RSL3-bound GPX4 and the apo (PDB code: 7L8K). Close-up view of the overlay depicting residues C66, L166-F170 in the apo structure (salmon) and RSL3-bound (light green). RSL3 and the residues are shown with stick models and labelled. Hydrogen bond is shown with a red dash line. **D**, Structure overlay of two apo GPX4 structures with PDB codes: 7L8K and 2OBI. Close-up view of the C-terminal residues (P167-F170) in 7L8K (in salmon) and 2OBI (yellow). Protomer B, in 2OBI, is shown in grey and residues in both structures are shown with stick models and labelled. Hydrogen bonds are shown with red dash lines. **E**, Structural overlay of two pseudo-trimers of apo and RSL3-bound. Protomer A of the apo structure (PDB code: 7L8K, in salmon) was superimposed onto that of RSL3-bound structure (light green). RSL3 and C66 are shown with stick models and the RSL3-bound protomers are labelled. Protomer B and C of the apo structure are shown in grey and purple, respectively. **F**, Chemical structure of RSL3-minus-Cl. **G**, Melting temperature changes of $GPX4^{U46C}$ with different concentrations of RSL3-minus-Cl in comparison to DMSO vehicle control, as measured in the thermal shift assay. Data are plotted as means ± s.d. (n = 3 biologically independent samples). **H**, Left panel: Representative sensorgrams of RSL3-minus-Cl at different concentrations as measured in the SPR binding assays with $GPX4^{U46C}$ immobilized on the sensor chip. Right panel: Response units of each concentration at equilibrium in the SPR sensorgrams were fitted with the Hill model. The data points are coloured based on the colour of corresponding response curve in the left panel. The experiments were performed in two biologically independent replicates. K_D = 60 ± 30 μM. **I**, Overlap of ^{1}H, ^{15}N-HSQC-NMR spectrum of 10 μM ^{15}N-$GPX4^{U46C}$ alone and its mixture with 1 mM RSL3-minus-Cl (both in 10.0 % d6-DMSO), with zoom-in panels on selected peaks of prominent changes.

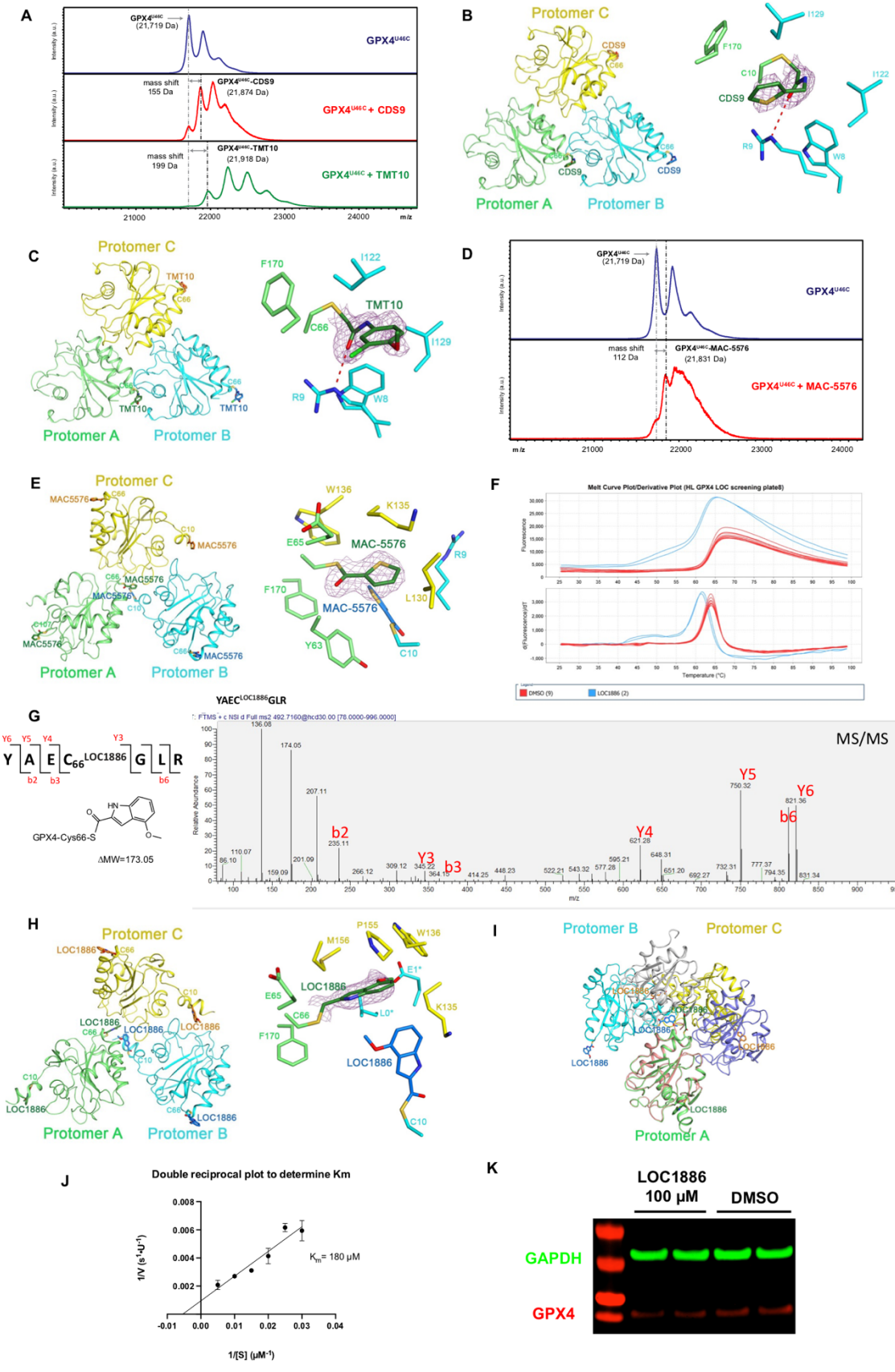
A
GPX4U46C (21,719 Da)
GPX4U46C
mass shift 155 Da
GPX4U46C-CDS9 (21,874 Da)
GPX4U46C + CDS9
mass shift 199 Da
GPX4U46C-TMT10 (21,918 Da)
GPX4U46C + TMT10
Intensity (a.u.)
21000
22000
23000
24000
m/z
B
Protomer C
CDS9
C66
Protomer A
Protomer B
I129
F170
C10
I122
R9
W8
C
Protomer C
TMT10
C66
Protomer A
Protomer B
F170
I122
TMT10
I129
R9
W8
D
GPX4U46C (21,719 Da)
GPX4U46C
mass shift 112 Da
GPX4U46C-MAC-5576 (21,831 Da)
GPX4U46C + MAC-5576
E
Protomer C
MAC5576
C66
C10
Protomer A
Protomer B
W136
K135
E65
MAC-5576
R9
F170
L130
Y63
F
Melt Curve Plot/Derivative Plot (HL GPX4 LOC screening plate8)
Fluorescence
Temperature (°C)
DMSO (9)
LOC1886 (2)
G
YAECLOC1886GLR
Y6 Y5 Y4 Y3
b2 b3 b6
GPX4-Cys66-S
ΔMW=173.05
MS/MS
Relative Abundance
m/z
b2
Y3
b3
Y4
Y5
Y6
b6
H
Protomer C
LOC1886
C66
C10
Protomer A
Protomer B
P155
M156
W136
E1*
E65
K135
L0*
F170
I
Protomer B
Protomer C
Protomer A
J
Double reciprocal plot to determine Km
1/V (s-1·U-1)
1/[S] (μM-1)
Km= 180 μM
K
LOC1886
100 μM
DMSO
GAPDH
GPX4

Supplemental Figure 5. Evaluation of GPX4 inhibitors with biophysical/biochemical assays and co-crystal structures, Related to Figure 5 and 6. A, Intact protein MALDI MS analysis of $GPX4^{U46C}$ preincubated with DMSO, CDS9, or TMT10. **B** and **C**, A cartoon representation of the three protomers of $GPX4^{U46C\text{-}R152H}$ in complex with CDS9 or TMT10 is shown in the panel on the left. The three protomers (light green, cyan, and yellow), the CDS9 or TMT10 molecule (dark green, marine, and orange), and the side chains of amino acids cys66 are shown with stick models and labeled. A close-up view of the CDS9 or TMT10 molecule at the interface of protomer A and protomer B was shown in the panel on the right, along with the side chains of residues that are involved in recognition of the CDS9 or TMT10 (dark green) from protomer A (light green). The Fo-Fc omit map, contoured at 3σ (in grey mesh), for the CDS9 or TMT10 molecule (dark green) from the protomer A (light green) is also shown and all the involved residues are labeled with respective color codes. A hydrogen bond, formed between the side chain of residue R9 (cyan) and the carbonyl group of CDS9 or TMT10 is shown with a red dash line. **D,** Intact protein MALDI MS analysis of $GPX4^{U46C}$ preincubated with DMSO or MAC-5576. **E**, A cartoon representation of the three protomers of $GPX4^{U46C}$ in complex with MAC-5576 is shown in the panel on the left. The three protomers (light green, cyan, and yellow), the MAC-5576 molecules (dark green, marine, and orange), and the side chains of amino acids cys10, cys66, and cys107 are shown with stick models and labeled. A close-up view of the two MAC-5576 molecules (dark green and marine) at the interface of protomer A and protomer B was shown in the panel on the right, along with the side chains of residues that are involved in recognition of the MAC-5576 (dark green) from protomer A (light green). The Fo-Fc omit map, contoured at 3σ (in grey mesh), for the MAC-5576 molecule (dark green) bound to cys66 in the protomer A (light green) is also shown and all the involved residues are labeled with respective color codes. We observed the best-defined electron density for MAC-5576 at cys66 site, which is followed by cys10 site. Only weak electron density of MAC-5576 was observed on cys107. **F**, Thermal shift assay on $GPX4^{U46C}$ of LOC1886 (blue), as compared to DMSO control (red). **G**, LC–MS/MS spectra of the LOC1886 modification of $GPX4^{U46C}$ at residue C66. In the LC-MS/MS analysis on trypsin digested $GPX4^{U46C}$-LOC1886 complex, the peptide containing Cysteine 66 (YAECGLR) was analyzed for mass shift induced by binding of LOC1886 (173.05). **H**, A cartoon representation of the three protomers of $GPX4^{U46C}$ in complex with LOC1886 is shown in the panel on the left. The three protomers (light green, cyan, and yellow), the LOC1886 molecules (dark green, marine, and orange), and the side chains of amino acids cys10 and cys66 are shown with stick models and labeled. A close-up view of the two LOC1886 molecules (dark green and marine) at the interface of protomer A and protomer B was shown in the panel on the right, along with the side chains of residues that are involved in recognition of the LOC1886 (dark green) from protomer A (light green). The Fo-Fc omit map, contoured at 3σ (in grey mesh), for the LOC1886 molecule (dark green) bound to cys66 in the protomer A (light green) is also shown and all the involved residues are labeled with respective color codes. **I**, A, Structural overlay of two pseudo-trimers of apo and LOC1886-bound. Protomer A of the apo structure (PDB code: 7L8K, in salmon) was superimposed onto that of LOC1886-bound structure (light green). LOC1886 and C66 are shown with stick models and the LOC1886-bound protomers are labelled. Protomer B and C of the apo structure are shown in grey and purple, respectively. **J**, Measurement of the K_m constant for $GPX4^{U46C}$ (n=2). Data are presented as mean ±

s.d. **K**, Native GPX4 in HT-1080 cells were tested for vulnerability to degradation induced by 100 μM LOC1886, as in a Western Blot assay (n=2).

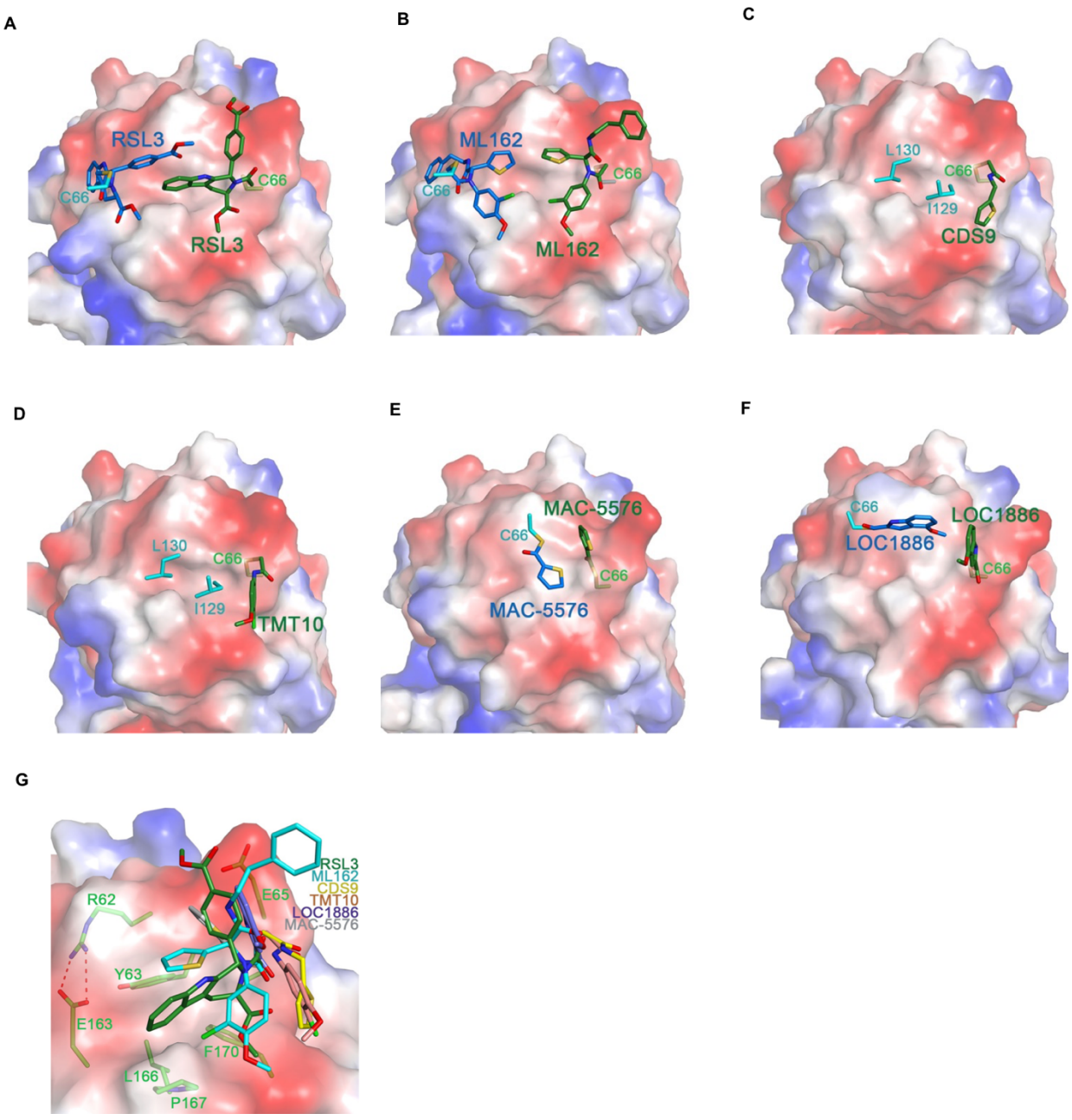

Supplemental Figure 6. Structural overlay of apo and inhibitor-bound GPX4 and electrostatic surface potential of GPX4 bound to inhibitors, Related to Figure 5. A, Surface potential of the GPX4^{U46C} protomer bound to RSL3. The RSL3 molecules and the side chain of cys66 from protomer B (cyan) are shown with stick models and the position of cys66 in protomer A (light green) is labeled. Negative, positive and neutral surface potential is highlighted in red, blue, and white, respectively. **B**, Surface potential of the GPX4$^{U46C\text{-}R152H}$ protomer bound to ML162. The ML162 molecules and the side chain of Cys-66 from protomer B (cyan) are shown with stick models and the position of

cys66 in protomer A is labeled (light green). **C**, Surface potential of the GPX4$^{U46C-R152H}$ protomer bound to CDS9. The CDS9 molecule and the side chains of I129 and L130 from protomer B (cyan) are shown with stick models and the position of cys66 in protomer A (light green) is labeled. **D**, Surface potential of the GPX4$^{U46C-R152H}$ protomer bound to TMT10. The TMT10 molecule and the side chain of I129 and L130 from protomer B (cyan) are shown with stick models and the position of cys66 in protomer A is labeled (light green). **E**, Surface potential of the GPX4^{U46C} protomer bound to MAC5576. The MAC5576 molecules and the side chain of cys10 from is labeled (light green). **F**, Surface potential of the GPX4^{U46C} protomer bound to LOC1886. The LOC1886 molecules and the side chain of cys10 from protomer B (cyan) are shown with stick models and the position of cys66 in protomer A is labeled (light green). **G**, Superposition of crystal structures of GPX4 bound to six different inhibitors bound to C66. Structural overlay was done on protomer A of GPX4 bound to RSL3. For the sake of clarity, the surface potential of the GPX4^{U46C} bound to RSL3 is only shown. All residues and inhibitors are depicted with stick models and labeled.

Supplemental Table 1. Crystallography data collection and refinement statistics, related to STAR Methods.

Protein	$GPX4^{U46C}$	$GPX4^{U46C-R152H}$	$GPX4^{U46C-R152H}$	$GPX4^{U46C-R152H}$	$GPX4^{U46C}$	$GPX4^{U46C}$
Inhibitor	**RSL3**	**ML162**	**CDS9**	**TMT10**	**MAC-5576**	**LOC1886**
Space group	$P2_1$	$C2$	$C2$	$C2$	$P2_1$	$C222_1$
Cell dimensions						
a, *b*, *c* (Å)	32.9, 92.9, 53.8	82.6, 69.3, 33.0	137.1, 36.6, 84.1	128.1, 36.6, 42.2	60.9, 91.5, 72.2	67.8, 115.7, 61.2
α, β, γ (°)	90, 100.2, 90	90, 102.5, 90	90, 115.5, 90	90, 101.3, 90	90, 90, 90	90, 90, 90
Resolution (Å)	28.63-1.60 (1.62-1.60)*	52.55-1.69 (1.73-1.69)*	75.90-1.91 (1.94-1.91)*	41.36-1.73 (1.77-1.73)*	72.19-2.25 (2.28-2.25)*	58.51-1.93 (1.98-1.93)*
R_{merge} (%)	5.1 (53.7)	10.1 (57.6)	19.9 (64.5)	23.7 (73.6)	19.7 (69.0)	13.0 (59.0)
I/σI	16.0 (2.2)	11.6 (1.8)	7.1 (1.8)	7.3 (1.7)	2.4 (1.9)	11.4 (2.2)
Completeness (%)	98.9 (93.1)	98.6 (93.3)	99.5 (99.7)	98.5 (85.1)	99.7 (85.0)	99.8 (100)
Redundancy	4.0 (3.0)	6.7 (4.7)	6.8 (6.7)	6.8 (5.4)	7.0 (7.2)	13.2 (11.7)
CC1/2	0.99 (0.90)	0.99 (0.88)	0.99 (0.91)	0.99 (0.82)	0.99 (0.84)	0.99 (0.89)
Refinement						
Resolution (Å)	26.7-1.60 (1.62-1.60)*	52.55-1.69 (1.73-1.69)*	75.90-1.91 (1.94-1.91)*	41.36-1.73 (1.77-1.73)*	72.19-2.25 (2.28-2.25)*	58.51-1.93 (1.98-1.93)*
No. reflections	41,412 (1,228)	20,242 (1,997)	29,453 (2,848)	19,999 (1,184)	37,533 (1,271)	18,477 (1,263)
R_{work} / R_{free} (%)	15.1 (24.7)/ 18.3 (27.0)	15.5 (25.0)/ 18.1 (28.6)	22.1 (30.7)/ 26.3 (35.0)	17.9 (29.8)/ 21.4 (35.3)	17.0 (21.4)/ 23.4 (29.6)	16.2 (24.3)/ 19.6 (27.2)
Ramachantran Plot (%)						
Outliers	0.00	0.00	0.00	0.00	0.00	0.00
Allowed	0.00	2.65	0.95	0.64	1.68	0.59
Favored	100	97.35	99.05	99.36	98.32	99.41
No. atoms						
Protein	2,641	1,350	2,614	1,299	5,331	1,374
Ligand/ion	60	30	20	14	56	26
Water	504	140	55	149	284	124
B-factors						
Protein	15.2	33.7	35.4	25.4	34.9	43.0
Ligand/ion	56.8	106.5	77.3	68.5	62.0	56.6
Water	31.7	45.0	38.5	39.4	38.8	48.1
R.m.s deviations						
Bond lengths (Å)	0.006	0.006	0.007	0.005	0.007	0.006
Bond angles (°)	0.8	0.9	0.8	0.8	1.0	0.9
PDB id:	7U4N	7U4K	7U4I	7U4J	7U4L	7U4M

*Highest resolution shell is shown in parenthesis.